

BER Analysis of IM/DD FSO System with APD Receiver Over Gamma-Gamma Turbulence

Milica I. Petković¹, Goran T. Đorđević¹,
Dejan N. Milić¹, Bata V. Vasic¹

Abstract: In this paper, the bit-error rate (BER) performance of intensity-modulated with direct detection (IM/DD) free space optical (FSO) system using the on-off keying (OOK) and avalanche photodiode (APD) receiver is analyzed. The intensity fluctuations of the received optical signal are modeled by gamma-gamma distribution, while both zero and nonzero inner scale models are observed. The total receiver noise includes APD shot noise and thermal noise. The BER expression is theoretically derived and numerical results are presented. The results illustrate the BER dependence on the turbulence strength, propagation path length, APD gain and noise temperature.

Keywords: Atmospheric turbulence, Avalanche photodiode, Free space optical communications, Gamma-gamma distribution, On-off keying.

1 Introduction

Free space optical (FSO) communication is license-free technique, which offers many advantages such as: easy of deployment, low cost, high security, wide bandwidth. Also, FSO represents a good solution for the “last mile” problem. Still, FSO deployment is limited by the existence of atmospheric turbulence, which appears as result of the refractive index variations due to random changes in atmospheric temperature, pressure and wind speed. Atmospheric turbulence causes rapid intensity fluctuations at the received signal, also known as fading or scintillation [1]. Many statistical models have been proposed in order to determine turbulence strength. Since the gamma-gamma model showed the good matching between theoretical and experimental data, it has been adopted as an appropriate model in wide range of turbulence conditions [1 – 4].

Commercial FSO systems usually apply the intensity-modulation with direct detection (IM/DD) and the on-off keying (OOK) scheme, since it is the simplest model for implementation and design. In [5], bit error rate (BER) of

¹Faculty of Electronic Engineering, University of Niš, 14 Aleksandra Medvedeva, 18000 Niš, Serbia;
E-mails: milicapetkovic86@gmail.com; goran@elfak.ni.ac.rs; dejan.milic@elfak.ni.ac.rs;
bata.vasic@silicon-studio.com

FSO system with IM/DD using OOK over K-distributed atmospheric turbulence channel was derived, which is convenient in strong turbulence conditions. The outage probability and channel capacity of the same FSO system has been analyzed in [6].

After direct detection at the receiver, an optical signal is converted to an electrical by photodetector. Above mentioned papers analyzed FSO systems with photodetectors using PIN photodiodes. The avalanche photodiodes (APDs) can be also used in optical receiver design since they can provide larger values of responsivity compared to PIN [7]. The FSO systems using subcarrier binary phase-shift keying and APD photodiode at the reception were observed in [8]. The BER performance of rectangular quadrature amplitude modulation FSO system with APD receiver over log-normal and gamma-gamma channel has been analyzed in [9].

In this paper, we observe FSO system with IM/DD and OOK in the case of APD receiver utilization. The atmospheric turbulence is modeled by gamma-gamma distribution. The effects of turbulence strength, for both zero and nonzero inner scale, are observed. The BER expression is theoretically derived and numerical results are presented. The impacts of APD shot noise and thermal noise are taken into account. The influence of turbulence strength, APD's gain, transmitted power, link distance and noise temperature are discussed.

2 System Model

Fig. 1 shows the FSO system using IM/DD with OOK and APD receiver. The information bits are first modulated by IM with OOK. The output of modulator is the laser beam, whose direction and size are determined by telescope at the transmitter. The telescope output is optical signal that is sent through atmospheric channel to the receiver. Transmission over atmospheric channel is damaged by turbulence, attenuation and geometric loss. At the receiver, laser beam is narrowed by telescope and forwarded to the APD photodetector. The APD converts an optical signal into electrical [10]. The decision which bit is sent finally can be made.

The optical signal at the input of the APD photodetector can be expressed as

$$r = axI, \quad (1)$$

where x represents the information „on“ or „off“ bit, a is the total link loss and I is normalized irradiance accounted for the intensity fluctuations due to atmospheric turbulence. Since the FSO system with OOK scheme is assumed, x is either 0 or $2P_t$, where P_t is the average transmitted optical power.

The atmospheric attenuation and geometric loss are described by total link loss given by [8, 9]

$$a = \frac{A}{\pi \left(\frac{\theta L}{2} \right)^2} e^{-\beta_v L}, \quad (2)$$

where β_v denotes the extinction coefficient, L is the link distance and θ is the angle of divergence in radians. The area of the receiver A equals to $A = \pi D^2/4$ where D represents the diameter of the receiver's aperture.

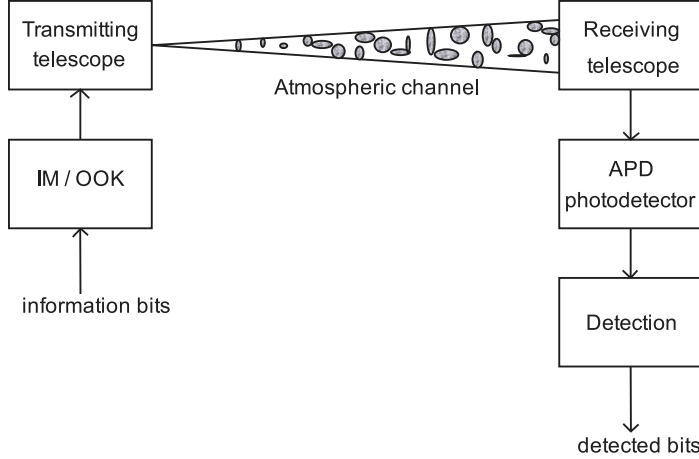


Fig. 1 – Block diagram of the FSO system using IM/OOK and APD receiver.

At the output of APD photodetector, electrical signal is different in „on“ or „off“ states and it is given by

$$r_e = \begin{cases} gRa2P_t I + n, & \text{"on"} \\ n, & \text{"off"} \end{cases} \quad (3)$$

where g and R represent the average gain and responsivity of APD, respectively. The total APD receiver noise n is caused by shot noise, thermal noise and dark current. If dark current is negligible, n can be expressed as [7 – 9]

$$n = i_{Th} + i_{Sh}, \quad (4)$$

where i_{Th} is the thermal noise and i_{Sh} the APD shot noise different in „on“ or „off“ states. The thermal noise can be modeled as stationary Gaussian random process with zero-mean and variance [7 – 9]

$$\sigma_{Th}^2 = 4k_B \frac{T}{R_L} F_n \Delta f, \quad (5)$$

where k_B denotes the Boltzmann constant, T is the receiver's temperature in degree Kelvin, R_L denotes APD's load resistance, F_n is the amplifier noise

figure and Δf is the symbol's effective noise bandwidth, here marked as $\Delta f = R_b/2$, where R_b is the bit rate.

In contrast to thermal noise, the shot noise depends on APD parts and it is different in „on“ and „off“ states. The shot noise can be modeled as stationary zero-mean Gaussian random process with variance [7]

$$\sigma_{Sh}^2 = \begin{cases} 2qg^2 F_A RaI2P_t \Delta f & \text{“on”} \\ 0 & \text{“off”} \end{cases} \quad (6)$$

where q is an electron charge and F_A denotes the excess noise factor of the APD given by

$$F_A = k_A g + (1 - k_A)(2 - 1/g), \quad (7)$$

where k_A is the ionization factor. The variance of the total APD noise can be expressed as [7]

$$\sigma_n^2 = \begin{cases} 4k_B \frac{T}{R_L} F_n \Delta f + 2qg^2 F_A RaI2P_t \Delta f, & \text{“on”} \\ 4k_B \frac{T}{R_L} F_n \Delta f, & \text{“off”} \end{cases} \quad (8)$$

3 Channel Model

The atmospheric channel is under the influence of atmospheric turbulence and attenuation and geometric loss. The atmospheric turbulence is modeled by gamma-gamma distribution given by [1-4]

$$p_I(I) = \frac{2(\alpha\beta)^{(\alpha+\beta)/2}}{\Gamma(\alpha)\Gamma(\beta)} I^{(\alpha+\beta)/2-1} K_{\alpha-\beta}(2\sqrt{\alpha\beta}I), \quad I \geq 0, \quad (9)$$

where $\Gamma(.)$ is the gamma function [11, (8.310.1)], $K_v(.)$ is the v th-order modified Bessel function of the second kind [11, (8.432)] and the parameters α and β represent the effective number of small-scale and large scale cells and can be related to the atmospheric conditions.

Free space optical signal is transmitted through medium, which can be comprehended as plenty of unstable individual cells of air or eddies of different diameters and refractive indices. According to theory about turbulence model, the atmospheric channel represents plenty of unstable large turbulent eddies characterized by outer scale L_0 . With increasing wind speed, at a certain point the kinetic energy from large eddies is transferred without loss to smaller turbulent eddies, which are characterized by the inner scale l_0 . If the inner scale is neglected, $l_0 = 0$, we have the zero inner scale. When nonzero inner scale is considered ($l_0 \neq 0$), the model needs to be modified in order to explain the slight

changes in the power spectrum of the refractive index variations. The parameters α and β can be determined depending on observed scale. In order to obtain their values, the strength of the turbulence is explained by the Rytov variance given by

$$\sigma_R^2 = 1.23 C_n^2 k^{7/6} L^{11/6}, \quad (10)$$

where $k=2\pi/\lambda$ is the wave-number, λ is the wavelength, L is the propagation distance, and C_n^2 denotes the weather and altitude dependent index of refraction structure. The index C_n^2 typically varies from 10^{-17} to $10^{-13} \text{ m}^{-2/3}$ and here it is used for determination of the turbulence strength.

When zero inner scale ($l_0 = 0$) and plane wave propagation are assumed, the parameters α and β are found as [1, 4]

$$\begin{aligned} \alpha &= \left(\exp \left[\frac{0.49 \sigma_R^2}{(1 + 1.11 \sigma_R^{12/5})^{7/6}} \right] - 1 \right)^{-1}, \\ \beta &= \left(\exp \left[\frac{0.51 \sigma_R^2}{(1 + 0.69 \sigma_R^{12/5})^{5/6}} \right] - 1 \right)^{-1}. \end{aligned} \quad (11)$$

In the case of nonzero inner scale ($l_0 \neq 0$) and plane wave propagation, the parameters α and β are [1, 4]

$$\begin{aligned} \alpha &= \left(\exp \left[\sigma_{\ln X}^2 \right] - 1 \right)^{-1}, \\ \beta &= \left(\exp \left[\frac{0.51 \sigma_p^2}{(1 + 0.69 \sigma_p^{12/5})^{5/6}} \right] - 1 \right)^{-1}, \end{aligned} \quad (12)$$

where $\sigma_{\ln X}^2$ is given by [1, 4]

$$\begin{aligned} \sigma_{\ln X}^2 &= 0.16 \sigma_R^2 \left(\frac{\eta_x Q}{\eta_x + Q} \right)^{\frac{7}{6}} \times \\ &\times \left[1 + 1.75 \left(\frac{\eta_x}{\eta_x + Q} \right)^{\frac{1}{2}} - 0.25 \left(\frac{\eta_x}{\eta_x + Q} \right)^{\frac{7}{12}} \right]. \end{aligned} \quad (13)$$

The remaining required parameters can be found as [1, 4]

$$\eta_x = \frac{2.61}{1 + 0.45 \sigma_R^2 Q^{1/6}}, \quad Q = \frac{10.89 L}{k l_0^2}, \quad (14)$$

$$\begin{aligned} \sigma_p^2 = 3.86\sigma_r^2 & \left\{ \left(1 + 1/Q^2\right)^{11/12} \left[\sin\left(\frac{11}{6}\tan^{-1}Q\right) + \right. \right. \\ & + \frac{1.51}{(1+Q^2)^{1/4}} \sin\left(\frac{4}{3}\tan^{-1}Q\right) - \\ & \left. \left. - \frac{0.27}{(1+Q^2)^{7/24}} \sin\left(\frac{5}{4}\tan^{-1}Q\right) \right] - 3.5Q^{5/6} \right\}. \end{aligned} \quad (15)$$

4 BER Analysis

In practice, the FSO systems usually employ IM/DD with OOK because its simplicity in design and implementation. However, there is need to set a threshold for detection, which is a major problem in this system realization.

The BER expression of FSO using IM/DD with OOK is calculated as [7]

$$P_e = P(1)P(0|1) + P(0)P(1|0), \quad (16)$$

where $P(1)$ and $P(0)$ represent the probabilities of transmitting „on“ and „off“ bits, respectively. The probability of detecting „off“ bit when „on“ bit is sent is $P(0|1)$, and $P(1|0)$ is the otherwise. It is considered that $P(1) = P(0) = 0.5$. Since the noise variance are different in „on“ and „off“ states, the probabilities $P(0|1)$ and $P(1|0)$ are not equal and they depend on decision threshold. So, the decision threshold effects on BER. Under condition that $P(0|1) = P(1|0)$, according to [7] the BER can be expressed as

$$P_{e/I} = \frac{1}{2} \operatorname{erfc}\left(\frac{Q(I)}{\sqrt{2}}\right), \quad (17)$$

where the parameter Q is

$$Q(I) = \frac{gRa2P_t I - 0}{\sigma_{n/on} + \sigma_{n/off}}. \quad (18)$$

The average BER over gamma-gamma fading channel is conditioned on I , so can be found as

$$P_e = \frac{1}{2} \int_0^\infty \operatorname{erfc}\left(\frac{gRa2P_t I}{\sqrt{2}(\sigma_{n/on} + \sigma_{n/off})}\right) p_I(I) dI. \quad (19)$$

After substituting (9) into (19) it follows:

$$P_e = \frac{(\alpha\beta)^{(\alpha+\beta)/2}}{\Gamma(\alpha)\Gamma(\beta)} \int_0^{\infty} I^{(\alpha+\beta)/2-1} K_{\alpha-\beta} \left(2\sqrt{\alpha\beta I} \right) \times \times \operatorname{erfc} \left(\frac{gRa2P_t I}{\sqrt{2} \left(\sqrt{4k_B \frac{T}{R_L} F_n \Delta f + 2qg^2 F_A Ra I 2P_t \Delta f} + \sqrt{4k_B \frac{T}{R_L} F_n \Delta f} \right)} \right) dI. \quad (20)$$

The final BER expression has no closed form and it is evaluated numerically.

5 Numerical Results

Numerical results obtained by derived expression are presented. The values of system parameters and constants are given in **Table 1** [8, 9]. According to turbulence strength, certain values of index refraction are: $C_n^2 = 6 \times 10^{-15}$ in weak, $C_n^2 = 2 \times 10^{-14}$ in moderate and $C_n^2 = 5 \times 10^{-14}$ in strong turbulence conditions [8]. The parameters α and β are determined by (11) for zero inner scale, and by (12) – (15) when nonzero inner scale is considered.

Table 1
Constants and system parameters.

NAME	SYMBOL	VALUE
Optical wavelength	λ	$1.55 \text{ }\mu\text{m}$
Boltzmann constant	k_B	$1.38 \times 10^{-23} \text{ W/kHz}$
Electron charge	q	$1.6 \times 10^{-19} \text{ C}$
APD load resistance	R_L	1000Ω
Amplifier noise figure	F_n	2
Bit rate	R_b	2 Gb/s
Ionization factor	k_A	0.7 (InGaAs)
Responsivity	R	1 A/W
Receiver's aperture diameter	D	0.02 m
Angle of divergence	θ	10^{-3} rad
Extinction coefficient	β_v	0.1 dB/km

BER dependence on the average APD gain for different propagation distances is shown in Fig. 2. The nonzero inner scale is considered. When propagation distance is greater, BER performance is worse. The system performance can be optimized by a proper selection of APD gain because the BER minimum exists. The appropriate selection of APD gain is very important in receiver design.

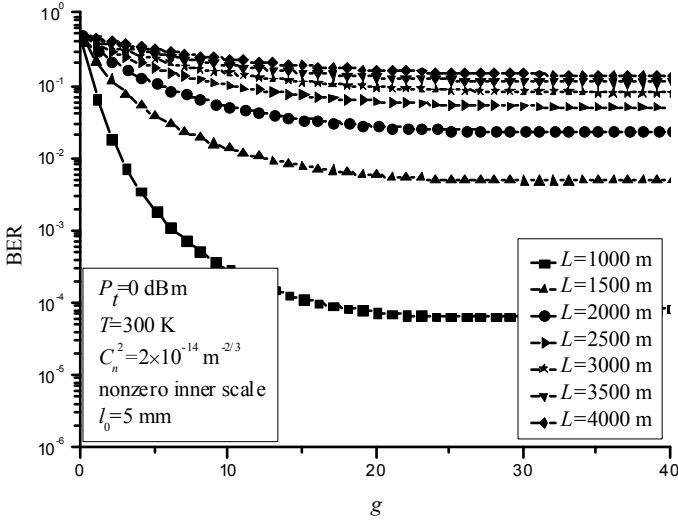


Fig. 2 – BER dependence on the average APD gain for different values of distance L when nonzero inner scale is considered.

The effect of the receiver noise temperature T for zero inner scale can be observed in Fig. 3. The system has better performance at lower temperatures T . With varying the value of temperature T , the optimal gain is changing rapidly. When $T = 300$ K the optimal gain is $g = 26.1$, and when $T = 700$ K we have $g = 32.1$. Also, when higher values of g , the effect of the receiver noise temperature on performance becomes less expressed.

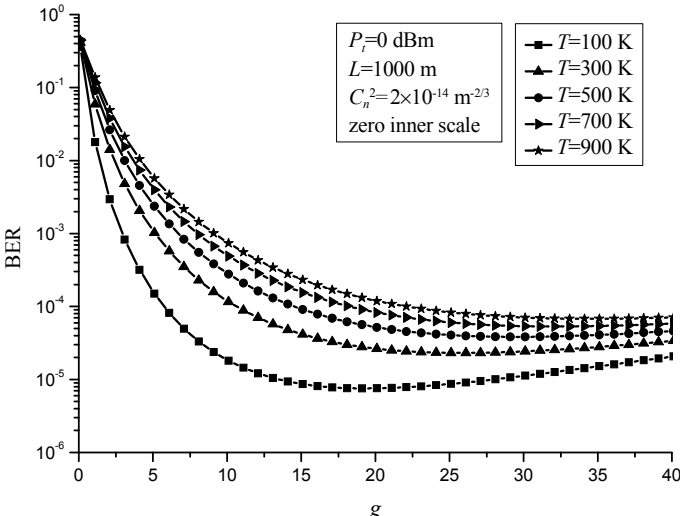


Fig. 3 – BER dependence on the average APD gain for different values of receiver noise temperature T when zero inner scale is considered.

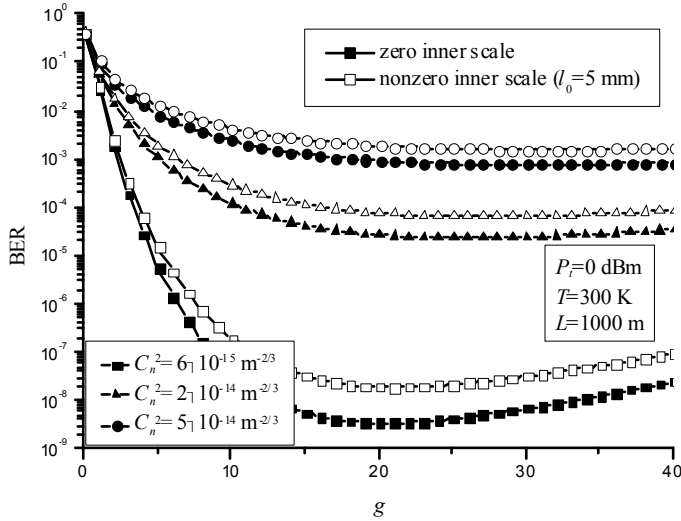


Fig. 4 – BER dependence on the average APD gain for different values of turbulence strength for both zero and nonzero inner scales.

In Fig. 4 BER dependence on g for different values of parameter C_n^2 is presented. The zero and nonzero scales are considered. As expected, the results illustrated that the system has better performance for lower values of C_n^2 (weak turbulence). The influence of APD gain is less expressed in strong turbulence conditions.

Next, the BER dependence on average transmitted power is presented while the average gain is $g = 10$. In Fig. 5, BER dependence for different values of propagation distance L for zero inner scale is shown. If the certain BER is wanted, the greater transmitted power is needed.

In Fig. 6, the same BER dependence is observed, while receiver noise temperature equals 300 K and 700 K. The nonzero inner scale is considered, when the inner scale values are 2 mm, 5 mm and 10 mm. System has better performance when the temperature is lower. Also, the degradation of BER performance is noticed with increasing inner scale value.

The same dependence in different atmospheric conditions is shown in Fig. 7. To achieve a certain value of BER, the greater transmitted power P_t is needed when C_n^2 is higher, i.e. in strong turbulence conditions. Besides the zero inner scale, nonzero inner scales with different values of inner scale are observed. With higher values of inner scale parameter, system has worse performance. The best performance are manifested when $l_0 = 0$, i.e. zero inner scale.

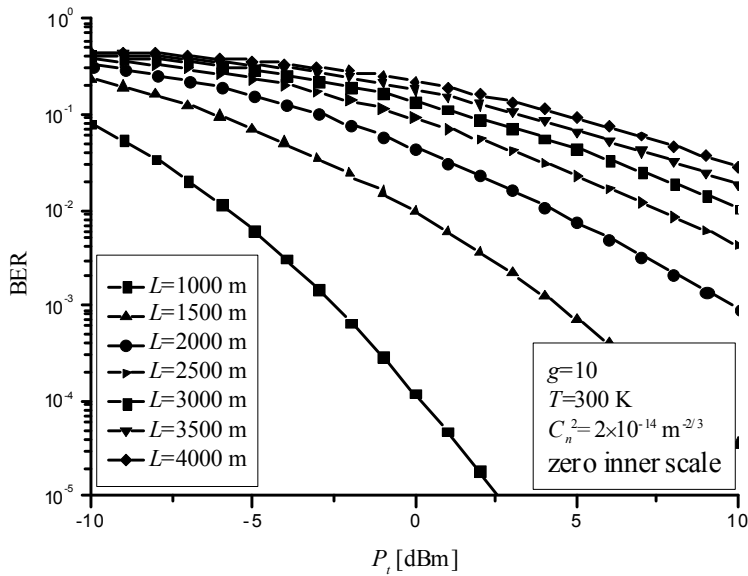


Fig. 5 – BER dependence on the average transmitted power P_t for different values of distance L when zero inner scale is considered.

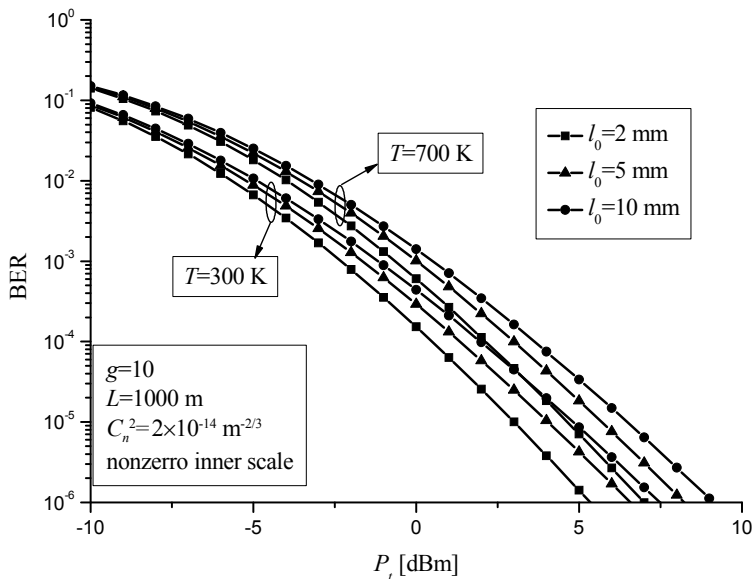


Fig. 6 – BER dependence on the average transmitted power P_t for different values of receiver noise temperature T when nonzero inner scale is considered.

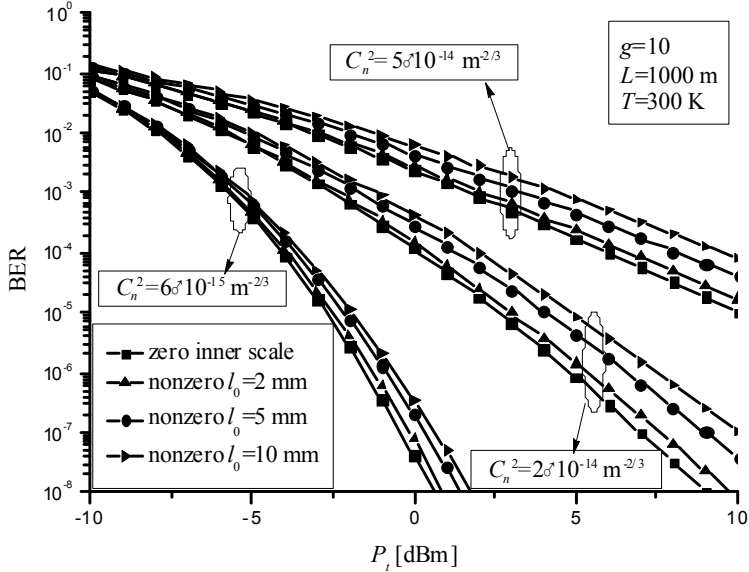


Fig. 7 – BER dependence on the average transmitted power P_t for different values of turbulence strength for both zero and nonzero inner scales.

6 Conclusion

In this paper, we observe the BER performance of FSO system using IM/DD with OOK and APD receiver. The atmospheric turbulence is modeled by gamma-gamma distribution which is an appropriate model in wide range of atmospheric conditions. Both zero and nonzero inner scales are considered. The receiver noise which includes APD shot noise and thermal noise is modeled as additive white Gaussian noise. The BER expression is derived and numerical results are presented, while the effects of various link conditions and receiver configurations are observed. With proper selection of the optimal APD's gain which depends on system conditions, system performance can be significantly improved.

7 Acknowledgement

This paper was supported in part by the Ministry of Science of Republic of Serbia under grants TR-32028 and III-44006 and in part by the Norwegian Ministry of Foreign Affairs under the project NORBAS (grant 2011/1383) headed by NTNU. The authors also acknowledge the ICT COST Action IC1101.

8 References

- [1] L.C. Andrews, R.L. Philips: *Laser Beam Propagation through Random Media*, SPIE Press, Bellingham, WA, USA, 2005.
- [2] T.A. Tsiftsis: Performance of Heterodyne Wireless Optical Communication Systems over Gamma-gamma Atmospheric Turbulence Channels, *Electronic Letters*, Vol. 44, No. 5, Feb. 2008, pp. 372 – 373.
- [3] M.A. Al-Habash, L.C. Andrews, R.L. Phillips: Mathematical Model for the Irradiance Probability Density Function of a Laser Beam Propagating through Turbulent Media, *Optical Engineering*, Vol. 40, No. 8, Aug. 2001, pp. 1554 – 1562.
- [4] J.A. Anguita, I.B. Djordjević, M.A. Neifeild, B.V. Vasic: Shannon Capacities and Error-correction Codes for Optical Atmospheric Turbulent Channels, *Journal of Optical Networking*, Vol. 4, No. 9, Sept. 2005, pp. 586 – 601.
- [5] T.A. Tsiftsis, H.G. Sandalidis, G.K. Karagiannidis, M. Uysal: Optical Wireless Links with Spatial Diversity over Strong Atmospheric Turbulence Channels, *IEEE Transactions on Wireless Communications*, Vol. 8, No. 2, Feb. 2009, pp. 951 – 957.
- [6] H.G. Sandalidis, T.A. Tsiftsis: Outage Probability and Ergodic Capacity of Free-space Optical Links over Strong Turbulence, *Electronics Letters*, Vol. 44, No. 1, Jan. 2008, pp. 46 – 47.
- [7] G.P. Agrawal: *Fiber-optic Communications Systems*, John Wiley and Sons, NY, USA, 2002.
- [8] D.A. Luong, T.C. Thang, A.T. Pham: Effect of Avalanche Photodiode and Thermal Noises on the Performance of Binary Phase-shift Keyingsubcarrier-intensity Modulation/free-space Optical Systems over Turbulence Channels, *IET Communications*, Vol. 7, No. 8, May 2013, pp. 738 – 744.
- [9] B.T. Vu, N.T. Dang, T.C. Thang, A.T. Pham: Bit Error Rate Analysis of Rectangular QAM/FSO Systems using an APD Receiver over Atmospheric Turbulence Channels, *Journal of Optical Communications and Networking*, Vol. 5, No. 5, May 2013, pp. 437 – 446.
- [10] S. Benameur, M. Kandouci, O. Boumediene, S. Taik, M. Bouzid, M. Oukli: An Optical WDM Link Simulation at 4•10 Gb/s with the COMSIS Software, *Serbian Journal of Electrical Engineering*, Vol. 6, No. 2, Nov. 2009, pp. 343 – 349.
- [11] I.S. Gradshteyn, I.M. Ryzhik: *Table of Integrals, Series and Products*, Academic Press, NY, USA, 2000.